HHS Public Access

Author manuscript

Dev Dyn. Author manuscript; available in PMC 2021 October 23.

Published in final edited form as:

Dev Dyn. 2015 January ; 244(1): 56–68. doi:10.1002/dvdy.24178.

SPATIOTEMPORAL MAPPING OF VASCULARIZATION AND INNERVATION IN THE FETAL MURINE INTESTINE

John Hatch[*], **Yoh-suke Mukouyama**[*,†]

[*]Laboratory of Stem Cell and Neuro-Vascular Biology, Genetics and Developmental Biology Center, National Heart, Lung, and Blood Institute, National Institutes of Health, Building 10/6C103, 10 Center Drive, Bethesda, MD 20892

Abstract

Background—In mice, the intestinal tube develops from the splanchopleure prior to embryonic day 9.5. Subsequent patterning of nerves and blood vessels is critical for normal digestive function. A hierarchical branching vascular network allows for efficient nutrient absorption, while the complex enteric nervous system regulates intestinal motility as well as secretion, absorption, and blood flow. Despite the well-recognized significance of these systems, the precise mechanisms by which they develop have not been clearly established in mammals.

Results—Using a novel whole-mount immunohistochemical protocol, we visualize the pattern of intestinal neurovascular development in mice between embryonic day 10.5 and birth. In particular, we focus on the development and remodeling of the enteric vascular plexus, the migration and organization of enteric neural crest-derived cells, and the integration of peripheral sympathetic nerves with the enteric nervous system. These correlative data lead us to hypothesize a functional interaction between migrating neural crest-derived cells and endothelial cells of the primary capillary plexus, as well as a subsequent interaction between developing peripheral autonomic nerves and differentiated neural crest-derived cells.

Conclusions—These studies provide useful anatomical data for continuing investigations on the functional mechanisms underlying intestinal organogenesis.

Keywords

Enteric development; enteric nervous system; enteric vasculature; whole-mount imaging

INTRODUCTION

In order to efficiently manage nutrient absorption and digestive processes, the vertebrate small intestine possesses a stereotypical, hierarchically branched vascular network as well as a complex enteric nervous system (ENS), known also as the “second brain.” Both systems are critical to normal digestion. However, the mechanisms underlying their patterning during embryonic development have not been thoroughly investigated in mammals.

[†]Author for correspondence: Tel: (301) 451-1663, FAX: (301) 480-1581, mukoyamay@mail.nih.gov.

The murine intestine initially forms via tubulogenesis of the splanchopleure between embryonic day (E)8 and E9.5. The splanchopleure consists of internal endoderm associated with splanchnic mesoderm from the lateral plate (Meier, 1980; Wilm et al., 2005; Noah et al., 2011). The mature intestine consists of the mesothelial serosa, circular and longitudinal smooth muscle layers, and the submucosal vascular plexus which lies above the mucosal epithelium of the lumen. The intestine is connected to the body wall by the mesentery, a double epithelial layer. Blood and lymphatic vasculature extend from the mesentery through the smooth muscle layers to supply the submucosal vascular plexus. In embryonic development, endoderm gives rise to the epithelium of the lumen, while intestinal smooth muscles, vascular endothelial cells, mural cells, and the serosa are derived from the mesodermal layer (Meier, 1980; Kiefer, 2003; Wilm et al., 2005). To better understand the stereotypical patterning of blood and lymphatic vasculature, three-dimensional imaging is necessary to construct a temporal map of vascular network formation.

The ENS, meanwhile, is entirely derived from the neural crest. Vagal neural crest-derived cells (NCDCs) form the majority of the small intestine ENS, while the sacral neural crest contributes primarily to the hindgut (Yntema and Hammond, 1954; Burns and Douarin, 1998; Burns and Le Douarin, 2001; Wang et al., 2011). In the adult, the ENS consists of interconnected ganglia with an outer myenteric plexus that lies between the circular and longitudinal intestinal muscles as well as an inner submucosal plexus. The mature murine ENS contains more than 1.2 million neurons including sensory, inter-, and motor neurons of at least 18 different subtypes (Young and Newgreen, 2001; Gianino et al., 2003; Hao and Young, 2009). This complex arrangement allows for management of homeostatic functions such as motility, secretion, and blood flow. Additionally, the ENS receives significant input from the central nervous system, including vagal afferent nerves as well as sympathetic and parasympathetic efferent fibers. While the ENS is capable of autonomous function, these connections are important for efficiently managing gut homeostasis. Significant research has been devoted to the vagal afferent innervation of the gut (Ratcliffe et al., 2006; Powley et al., 2011; Ratcliffe, 2011; Ratcliffe et al., 2011a; Ratcliffe et al., 2011b), but the developing enteric sympathetic nervous system is less well understood.

The complexity of the enteric vasculature and neural circuitry raises the possibility that neurovascular interactions may play an important developmental role in the patterning of the intestine. Elucidating these interactions may reveal novel mechanisms of molecular communication between nerves and blood vessels not previously found in other tissues. To investigate the possibility of such mechanisms, we sought to visualize the patterning of vascular and neural systems on an organ-wide scale. Previous methods of visualizing molecular markers in high resolution, such as section immunohistochemistry or *in situ* hybridization, are inadequate for this goal as they cannot easily obtain spatiotemporal patterning data in three dimensions. In this study, we develop a novel whole-intestine immunohistochemical protocol to examine the timeline of development for both systems. High-resolution confocal microscopy allows three-dimensional visualization of numerous molecular markers that have been previously confined to section immunohistochemistry. With this data, we propose that ENS progenitors receive signals from capillary endothelial cells during migration, as has previously been suggested in avians (Nagy et al., 2009). At

later stages, the developing sympathetic innervation of the ENS appears to be mediated first by remodeled arteries and subsequently by ENS neurons or glial cells.

RESULTS AND DISCUSSION

Whole-mount immunohistochemistry reveals fetal intestinal development in three dimensions

In order to examine enteric development in detail, we established an immunohistochemical protocol that allows detailed visualization of intestinal development in three dimensions. Existing methods for developmental imaging, such as section immunohistochemistry, are insufficient to easily inspect organ-wide patterning processes during organogenesis. To adequately visualize the whole intestine, we developed a novel protocol to compensate for the unique challenges associated with the gut. In particular, the characteristically contorted structure of the intestine *in vivo* increases the difficulty of imaging all segments of the small intestine in a single sample, as in Fig. 3A. Thus, for samples older than E11.5, whole intestines were dissected immediately after sacrifice and soaked in PBS to relax the convolutions prior to fixation as well as after the final antibody incubation step. Additionally, the thickness of the intestine at stages past E15.5 reduces antibody penetration, requiring lengthened permeabilization and antibody incubation steps with the detergent Triton X-100. With this protocol, it is possible to visualize a wide variety of molecular markers throughout the gut, from the mesentery to the lumen (Figs. 1–9).

Endothelial cells sprout to form a primary capillary plexus between E9.5-E11.5.

In order to evaluate the potential for neurovascular interaction in the developing gut, we first produced a detailed temporal map of the patterning of enteric vasculature. Immunohistochemical staining with antibodies to platelet endothelial cell adhesion molecule 1 (PECAM1) reveals that vascular endothelial cells begin to sprout immediately following tubulogenesis. At E9.5, $PECAM1^+$ endothelial tubes are detectable in the proximal half of the intestine (Fig. 1A). In the distal intestine, endothelial cells sprout to occupy the remainder of the tissue (Fig. 1A', open arrowheads). There is a large aggregate of $PECAM1^+$ cells associated with mesodermal tissue present adjacent to the region containing endothelial sprouts (Fig. 1A', arrows). By E10.5, the intestine begins to fold at the region which will become the cecum, separating the small and large intestines (Fig. 1B). In the small intestine, the primary capillary plexus has been effectively established, while some endothelial sprouts are still detectable in the distal portion of the large intestine (Fig. 1B', open arrowheads). The large $PECAM1^+$ aggregation is still present (Fig. 1B', arrows), although with reduced size and signal intensity that may reflect that primary colonization of the intestine by endothelial cells is nearing completion.

The enteric vascular plexus remodels between E11.5-E15.5

Following primary vascularization, the intestine displays a uniform submucosal capillary plexus at E11.5 (Fig. 2A–A"). This network reorganizes to form the characteristic, hierarchically branched enteric vasculature by E15.5. Between E12.5 and E15.5, the intestine continues to increase in length and diameter and separates from the superior mesenteric artery (SMA) and superior mesenteric vein (SMV), which are co-localized

between the fore- and hind-gut. The intestinal vasculature remains connected to the SMA and SMV via remodeled vessels found between the layers of the growing mesentery. These vessels form via angiogenic remodeling and later become the inferior pancreaticoduodenal (supplying the duodenum) and intestinal (supplying the jejunum and ileum) arteries and veins (Fig. 2B' and C', open arrowheads). Vasa recta, arteries perpendicular to the intestinal wall which directly supply the submucosal vasculature, become visible in the duodenum and jejunum by E13.5 (Fig. 2B" and C", arrows). These are the first vessels to appear in the intestine that exist outside the submucosal layer; these vessels connect to mesenteric vessels in the subserosa and penetrate through intestinal muscle layers to supply the submucosal vasculature. Intestinal arteries and vasa recta are not distinguishable at E11.5 (Fig. 2A' and A", arrows).

By E15.5, the intestinal vasculature adopts a characteristic hierarchical pattern (Fig. 3A–A"), despite significant growth requirements between that stage and birth. At this stage, arteries and veins can be clearly distinguished by both morphology and expression of characteristic markers such as ephrinB2 (arteries) and EphB4 (veins) (Fig. 3A' and A", arteries indicated by arrows; veins indicated by open arrowheads; Fig. 3B–E). External vasa recta are readily identified along the length of the small intestine (Fig. 3A') and branch into the submucosal layer. Taken together, these studies demonstrate that the primary capillary network undergoes extensive angiogenic remodeling and develops into a hierarchical vascular branching network that expresses both arterial and venous markers.

Remodeling of intestinal arteries correlates with the recruitment of pericytes and vascular smooth muscle cells

The recruitment of mural cells such as vascular smooth muscle cells (VSMCs) and pericytes to developing vasculature is an important step in angiogenic remodeling (Folkman and D'Amore, 1996; Mukouyama et al., 2002; Nam et al., 2013). As these cells have been shown to guide sympathetic axons alongside blood vessels (reviewed in (Glebova and Ginty, 2005), the timing of their appearance in the intestinal vasculature is of significant interest. At E12.5, neural/glial antigen 2-positive ($NG2^+$) and alpha-smooth muscle actin-positive (αSMA^+) mural cells begin to appear in the developing mesentery (Fig. 4D). These cells surround intestinal arteries such that by E15.5, intestinal arteries from the SMA to the vasa recta are uniformly ensheathed, compared to little or no coverage of veins or the microvasculature in the intestinal submucosa (Fig. 4A–C, arteries indicated by arrows; Fig. 4D–F arteries indicated by arrows; veins indicated by open arrowheads). Due to the smooth muscle layers of the intestinal wall, vascular smooth muscle αSMA is not clearly distinguishable in the duodenum. Taken together, these observations suggest that any neurovascular interaction prior to E13.5 must depend on capillary endothelial cells rather than remodeled vessels, pericytes, or VSMCs. In contrast, neural patterning after E13.5 may depend on mural cell-derived signals.

Lymphatic vasculature expands from the mesentery beginning at E13.5

The intestinal lymphatic vasculature is critical to immune and homeostatic functions of the intestine (Miller et al., 2010). Importantly, the lymphatic vasculature develops at a different stage and in a distinct pattern from the blood vasculature (Kim et al., 2007). Lymphatic

markers are not detectable in the mesentery or the intestinal wall during the formation of the primary capillary plexus or at the initiation of venous and arterial remodeling (Kim et al., 2007). Immunohistochemical staining for lymphatic vessel endothelial hyaluronan receptor 1 (LYVE1) reveals rare lymphatic branches and tissue macrophages in the duodenal submucosa at E13.5 (Fig. 5A–A', lymphatic vessels indicated by arrows; tissue macrophages indicated by arrowheads). At E14.5 and E15.5, additional lymphatic vessels sprout adjacent to the mesenteric vasculature and vasa recta (Fig. 5B–B', lymphatic vessels indicated by arrows; remodeled blood vessels indicated by open arrowheads). By E16.5, lymphatics surround all major vessels in the submucosa of the duodenum (Fig. 5C–C'). Distinct from the blood vasculature, lymphatic endothelial cells appear first adjacent to the SMA at E13.5 and subsequently sprout along remodeled intestinal vessels (Fig. 5D). Interestingly, despite the expansion of lymphatics from the center of the mesentery, vessels first reach the duodenum at E13.5 but rarely reach the ileum prior to E15.5. This process parallels the proximal-to-distal pattern of angiogenic remodeling, suggesting that remodeled vessels may play a functional role in lymphatic development.

Neural crest-derived cell migration follows the formation of an enteric capillary plexus and precedes angiogenic remodeling

In order to evaluate the potential for a vascular role in neural crest-derived cell (NCDC) migration, we seek to correlate the timing of NCDC appearance in the gut with the development of the intestinal vasculature. This interaction has been previously demonstrated in avians (Nagy et al., 2009). Previous studies have characterized a number of genes associated with NCDC migration, including genes involved with the Ret signaling pathway such as *Ret* or *Gdnf* and transcriptional regulators of those genes, including *Phox2b* or *Sox10* (reviewed in (Heanue and Pachnis, 2007). However, many of these studies focus primarily on intrinsic functions of NCDCs rather than extrinsic signals that may influence the development and organization of the ENS. NCDCs express the low-affinity neurotrophin receptor (P75) throughout the process of migration and differentiation (Bernd, 1986; Smith-Thomas and Fawcett, 1989; Heuer et al., 1990). Undifferentiated $P75^{+}$ NCDCs migrate along the esophagus and stomach to arrive in the duodenum immediately after tubulogenesis and neovascularization, prior to E10.5. Between E10.5 and E11.5, NCDCs colonize the remainder of the small intestine (Fig. 6A–B). By E12.5, NCDCs begin to reach the distal portion of the colon (Fig. 6C). Importantly, NCDCs arrive at each region of the intestine rapidly following the (Heuer et al., 1990) formation of the primary capillary plexus, but prior to any detectable angiogenic remodeling. Primary NCDC migration therefore may involve endothelial cell-derived signals, but does not require signals from remodeled vessels or mural cells such as VSMCs or pericytes. High-resolution imaging reveals that migrating NCDCs are found in close apposition with capillary endothelial cells (Fig. 6A'–B'; NCDCs indicated by arrows; capillary endothelial cells indicated by open arrowheads). However, it is clear that NCDCs migrate outside of the submucosal vascular layer (Fig. 6C', arrows and open arrowheads). This data suggests that capillaries may contribute soluble factors necessary for NCDC migration, but direct contact between migrating ENS progenitors and endothelial cells may not be required.

NCDCs differentiate into enteric neurons and glia prior to organization into enteric ganglia

The enteric nervous system is comprised of a large number of distinct neuronal subtypes as well as glial cells. However, migrating NCDCs express few markers for differentiated cell types. We therefore seek to clarify the pattern of emergence for progenitor and mature neuronal and glial markers in order to provide insight into the process of ENS differentiation. A subset of migrating NCDCs expresses the transcription factor Phox2b, a marker for neural progenitors which is required for ENS formation (Fig. 7A–C). At E10.5 and E11.5, only a small fraction of these cells express neuronal class III β-tubulin (TuJ1), a marker for differentiated neurons (Fig. 7A). By E13.5, all $Phox2b^+$ NCDCs are also $TuJ1^+$ (Fig. 7B). At this stage, enteric neurons form a uniform network in the myenteric plexus with dispersed cell bodies and no obvious ganglia. No neuronal markers are yet detectable in the submucosal layer (data not shown). Between E13.5 and E17.5, myenteric neurons reorganize to form recognizable enteric ganglia connected by axon bundles (Fig. 7C). During the same period, axons extend medially into the submucosal layer to form a submucosal nerve plexus, and axons innervate developing villi (data not shown). None of these structures appear to be directly associated with the enteric vasculature.

Brain fatty acid-binding protein (BFABP), a marker for glial cells, becomes detectable by E13.5 (Fig. 7E), the same period at which neuronal precursors begin to differentiate and express mature neuronal markers. These $BFABP^+$ glia associate first with isolated neurons and can later be found associated primarily with enteric ganglia (Fig. 7F). As the majority of ENS interneurons are not myelinated, the lack of glia associated with interganglion axon bundles is expected. Notably, it remains unclear whether neurons and glia are specified prior to or during migration or whether the microenvironments found after migration may influence their differentiation.

Sympathetic nerves follow intestinal arteries to integrate with the existing enteric nerve plexus

While the ENS processes many local stimuli autonomously, there is significant input from the peripheral autonomic nervous system. Considerable investigation has elucidated the vagal afferent innervation that is critical for gut homeostasis (reviewed in (Powley et al., 2011; Ratcliffe, 2011; Ratcliffe et al., 2011b). However, the enteric sympathetic nervous system is less well characterized despite considerable input to a variety of cells in the gut including secretory cells, arteries, and enteric ganglia. Tyrosine hydroxylase $(TH)^+$ and $TuJ1^+$ sympathetic nerves are detectable adjacent to the SMA by E13.5 (Fig. 8A, open arrowhead), and subsequently extend along intestinal arteries and vasa recta to reach the myenteric nerve plexus by E15.5 (Fig. 8B–C, open arrowheads). Previous studies have characterized sympathetic axon guidance by arterial VSMCs in a variety of tissues (reviewed in (Glebova and Ginty, 2005). Defined molecular signals include Artemin (Enomoto et al., 2001; Honma et al., 2002), neurotrophin 3 (NT-3) (Francis et al., 1999; Kuruvilla et al., 2004), nerve growth factor (NGF) (Nam et al., 2013), and endothelins (Makita et al., 2008). Sympathetic axon extension in the mesentery begins immediately following the recruitment of VSMCs to arteries during angiogenic remodeling (Fig. 4D–F). It is therefore plausible that arterial VSMCs coordinate extension of sympathetic axons in the mesentery, although further experiments will be necessary to confirm this hypothesis. Notably, sympathetic axons

begin to innervate intestinal arteries postnatally (Brunet et al., 2014), but no axon endpoints can be seen in arteries as late as E17.5. This suggests two possible mechanisms for enteric sympathetic innervation. First, arteries may secrete only guidance signals prenatally and begin to produce neurotrophins for innervation at birth. Alternately, a distinct population of sympathetic nerves with different neurotrophin receptors may extend along and innervate intestinal arteries after E18.5 (Brunet et al., 2014). In either case, the first TH^+ axons to reach the gut all extend into the myenteric nerve plexus.

Interestingly, upon reaching the myenteric plexus prior to E15.5, enteric sympathetic nerves immediately defasciculate and abandon vasa recta to follow existing enteric nerves and ganglia (Fig. 8C, arrows). By E17.5, TH^+ fibers are detectable throughout the myenteric plexus, with especially strong signals around enteric ganglia (Fig. 8D and E, arrows). This behavior suggests active recruitment of sympathetic fibers by the ENS. In *Phox2b*$^{-/-}$ mice lacking an ENS (Pattyn et al., 1999), a few surviving sympathetic nerves continue to follow vasa recta into the deeper submucosal plexus (Fig. 9B, open arrowheads). It should be noted that *Phox2b*$^{-/-}$ mice have defects in the sympathetic nervous system leading to reduced numbers of sympathetic neurons, which is reflected in the reduced TH signal intensity in mutants (Fig. 9A'–B', open arrowheads). However, the capacity of vasa recta to guide TH^+ axons beyond the serosal layer in mutants indicates that defasciculation in wild-type animals (Fig 9A–A', arrows) is an active process that depends on the ENS. Whether this interaction is mediated by enteric neurons or glia remains to be clarified. Previous studies have shown that enteric neuron-derived netrins attract vagal afferent neurons during the same period (Ratcliffe et al., 2011a), and sympathetic neurons may respond to these or different neuron-derived signals. Further, sympathetic axons follow existing interganglion axon bundles, which have few or no glia, providing evidence for enteric neuron-mediated sympathetic axon guidance. However, other studies have shown that sympathetic axons target glia in the mammalian colon (Gulbransen et al., 2010). Thus, either cell type or both may contribute to the integration of the sympathetic nervous system with the ENS.

Neurovascular wiring in the developing gut

Our thorough anatomical and histological analysis of enteric vascular and neuronal development reveals a number of sequential processes whose underlying molecular mechanisms merit further study. First, our correlative data paired with previous studies in avians suggest that primary vascularization is required for NCDC migration (Fig. 10A). At later stages, sympathetic axon extension along intestinal arteries may be mediated by one of many signals that have been previously described for arterial-sympathetic interaction in other tissues (Fig. 10B). Finally, sympathetic innervation of enteric ganglia may be controlled by netrins, like vagal innervation of the intestine, or this neuronal interaction may be governed by a distinct mechanism that has not yet been described (Fig. 10C). Although further experiments are required to draw definitive conclusions regarding underlying mechanisms, our protocol provides a valuable tool that facilitates the exploration of these and other developmental processes during intestinal neurovascular patterning.

EXPERIMENTAL PROCEDURES

Experimental animals

The characterizations of *ephrinB2*$^{taulacZ/+}$ mice (Wang et al., 1998) and *EphB4*$^{taulacZ/+}$ mice (Gerety et al., 1999), *phox2b*$^{-/-}$ mice (Pattyn et al., 1999) have been reported elsewhere. Wild-type animals were bred from a C57BL6 background. All experiments were carried out according to the guidelines approved by Animal Care and Use Committee at NHLBI.

Whole-mount immunohistochemistry of embryonic intestines

Fetal intestines were processed differently depending on the stage of the sample. Prior to E12.5, whole embryos were fixed in 4% paraformaldehyde/PBS overnight at 4 °C. Intestines were subsequently dissected and stained according to the protocol below. At E12.5 and older, fresh embryos were dissected and intestines were allowed to soak in PBS for 1 hour at room temperature to relax the convolutions found *in vivo.* Individual intestines were fixed in 1 mL of 4% paraformaldehyde/PBS overnight at 4 °C. Fixed intestines were washed 3×5’ in PBS and then treated with a blocking/permeabilization buffer containing 10% heat-inactivated goat serum (HIGS)/PBS + 0.2% Triton X-100 (Sigma) for 2 hours at room temperature. Samples older than E15.5 were treated for 3–4 hours. Samples were incubated with primary antibodies diluted to appropriate concentrations (Table 1) in 1 mL of blocking/permeabilization buffer overnight (minimum 12 hours) at 4 °C. The following day, samples were washed in 2% HIGS/PBS + 0.2% Triton X-100 for 5×20’. Samples were then incubated overnight at 4 °C with secondary antibodies diluted to 1:250 in 1 mL of blocking/permeabilization buffer. Different combinations of Alexa-488-, Alexa-568-, Cy3- or Dylight 647-conjugated secondary antibodies (Invitrogen or Jackson) were used as appropriate to visualize each primary antibody. The secondary antibody solution was passed through a 0.22 μm filter syringe (Millex) to reduce non-specific signals. Prior to mounting, samples were washed again in 2% HIGS/PBS + 0.2% Triton X-100 for 5×20’. Finally, samples were prepared for imaging under a dissecting microscope by removing remnants of the pancreas, stomach, or colon that remained from primary dissection. For samples at E10-E12.5, the whole gut (duodenum-colon) was mounted directly on a 1 mm microscope slide (Tru Scientific). For E13-E16, the colon was removed and the small intestine (duodenum-ileum) was mounted similarly. For samples older than E16, the small intestine was divided in half at the jejunum and each segment was mounted on a slide inside a 0.5 mm spacer (Invitrogen). All samples were mounted in a minimal amount of ProlongGold (Life Technologies) and covered with 25×25 mm cover glass (Fisher) to preserve fluorescence intensity. All confocal analysis was conducted within two weeks of mounting on a Leica TCS SP5 confocal microscope (Leica).

ACKNOWLEDEGEMENTS

We thank J. F. Brunet for providing the anti-Phox2B antibody, T. Müller for providing the anti-BFABP antibody, and B. Stallcup for providing the anti-NG2 antibody. We also thank members of the Laboratory of Stem Cell and Neuro-Vascular Biology for technical help and thoughtful discussion. Thanks to R. S. Balaban and R. S. Adelstein for invaluable help and discussion. Thanks also to J. Hawkins and the staff of NIH Bldg50 animal facility for assistance with mouse breeding and care, K. Gill for laboratory management and technical support, and R. Reed and F. Baldrey for administrative assistance. None of the authors have any financial or other conflicts of interest. This work was supported by the Intramural Research Program of the National Heart, Lung, and Blood Institute, National Institutes of Health (NIH HL005702-07).

Grant sponsor and numbers: the Intramural Research Program of the National Heart, Lung, and Blood Institute, National Institutes of Health (NIH HL005702-07 for Y.M.)

REFERENCES

Bernd P 1986. Characterization of nerve growth factor binding to cultured neural crest cells: evidence of an early developmental form of the NGF receptor. Dev Biol 115:415–424. [PubMed: 3011567]

Brunet I, Gordon E, Han J, Cristofaro B, Broqueres-You D, Liu C, Bouvree K, Zhang J, Del Toro R, Mathivet T, Larrivee B, Jagu J, Pibouin-Fragner L, Pardanaud L, Machado MJ, Kennedy TE, Zhuang Z, Simons M, Levy BI, Tessier-Lavigne M, Grenz A, Eltzschig H, Eichmann A. 2014. Netrin-1 controls sympathetic arterial innervation. J Clin Invest 124:3230–3240. [PubMed: 24937433]

Burns AJ, Douarin NM. 1998. The sacral neural crest contributes neurons and glia to the post-umbilical gut: spatiotemporal analysis of the development of the enteric nervous system. Development 125:4335–4347. [PubMed: 9753687]

Burns AJ, Le Douarin NM. 2001. Enteric nervous system development: analysis of the selective developmental potentialities of vagal and sacral neural crest cells using quail-chick chimeras. Anat Rec 262:16–28. [PubMed: 11146425]

Enomoto H, Crawford PA, Gorodinsky A, Heuckeroth RO, Johnson EM Jr., Milbrandt J. 2001. RET signaling is essential for migration, axonal growth and axon guidance of developing sympathetic neurons. Development 128:3963–3974. [PubMed: 11641220]

Folkman J, D'Amore PA. 1996. Blood vessel formation: what is its molecular basis? Cell 87:1153–1155. [PubMed: 8980221]

Francis N, Farinas I, Brennan C, Rivas-Plata K, Backus C, Reichardt L, Landis S. 1999. NT-3, like NGF, is required for survival of sympathetic neurons, but not their precursors. Developmental Biology 210:411–427. [PubMed: 10357900]

Gerety SS, Wang HU, Chen ZF, Anderson DJ. 1999. Symmetrical mutant phenotypes of the receptor EphB4 and its specific transmembrane ligand ephrin-B2 in cardiovascular development. Molecular Cell 4:403–414. [PubMed: 10518221]

Gianino S, Grider JR, Cresswell J, Enomoto H, Heuckeroth RO. 2003. GDNF availability determines enteric neuron number by controlling precursor proliferation. Development 130:2187–2198. [PubMed: 12668632]

Glebova NO, Ginty DD. 2005. Growth and survival signals controlling sympathetic nervous system development. Annual Review of Neuroscience 28:191–222.

Gulbransen BD, Bains JS, Sharkey KA. 2010. Enteric glia are targets of the sympathetic innervation of the myenteric plexus in the guinea pig distal colon. J Neurosci 30:6801–6809. [PubMed: 20463242]

Hao MM, Young HM. 2009. Development of enteric neuron diversity. J Cell Mol Med 13:1193–1210. [PubMed: 19538470]

Heanue TA, Pachnis V. 2007. Enteric nervous system development and Hirschsprung's disease: advances in genetic and stem cell studies. Nat Rev Neurosci 8:466–479. [PubMed: 17514199]

Heuer JG, von Bartheld CS, Kinoshita Y, Evers PC, Bothwell M. 1990. Alternating phases of FGF receptor and NGF receptor expression in the developing chicken nervous system. Neuron 5:283–296. [PubMed: 2169268]

Honma Y, Araki T, Gianino S, Bruce A, Heuckeroth R, Johnson E, Milbrandt J. 2002. Artemin is a vascular-derived neurotropic factor for developing sympathetic neurons. Neuron 35:267–282. [PubMed: 12160745]

Kiefer JC. 2003. Molecular mechanisms of early gut organogenesis: a primer on development of the digestive tract. Dev Dyn 228:287–291. [PubMed: 14518001]

Kim KE, Sung HK, Koh GY. 2007. Lymphatic development in mouse small intestine. Dev Dyn 236:2020–2025. [PubMed: 17576138]

Kuruvilla R, Zweifel LS, Glebova NO, Lonze BE, Valdez G, Ye H, Ginty DD. 2004. A neurotrophin signaling cascade coordinates sympathetic neuron development through differential control of TrkA trafficking and retrograde signaling. Cell 118:243–255. [PubMed: 15260993]

Makita T, Sucov HM, Gariepy CE, Yanagisawa M, Ginty DD. 2008. Endothelins are vascular-derived axonal guidance cues for developing sympathetic neurons. Nature 452:759–763. [PubMed: 18401410]

Meier S 1980. Development of the chick embryo mesoblast: pronephros, lateral plate, and early vasculature. J Embryol Exp Morphol 55:291–306. [PubMed: 7373199]

Miller MJ, McDole JR, Newberry RD. 2010. Microanatomy of the intestinal lymphatic system. Ann N Y Acad Sci 1207 Suppl 1:E21–28. [PubMed: 20961303]

Mukouyama YS, Shin D, Britsch S, Taniguchi M, Anderson DJ. 2002. Sensory nerves determine the pattern of arterial differentiation and blood vessel branching in the skin. Cell 109:693–705. [PubMed: 12086669]

Nagy N, Mwizerwa O, Yaniv K, Carmel L, Pieretti-Vanmarcke R, Weinstein BM, Goldstein AM. 2009. Endothelial cells promote migration and proliferation of enteric neural crest cells via beta1 integrin signaling. Dev Biol 330:263–272. [PubMed: 19345201]

Nam J, Onitsuka I, Hatch J, Uchida Y, Ray S, Huang S, Li W, Zang H, Ruiz-Lozano P, Mukouyama YS. 2013. Coronary veins determine the pattern of sympathetic innervation in the developing heart. Development 140:1475–1485. [PubMed: 23462468]

Noah TK, Donahue B, Shroyer NF. 2011. Intestinal development and differentiation. Exp Cell Res 317:2702–2710. [PubMed: 21978911]

Pattyn A, Morin X, Cremer H, Goridis C, Brunet JF. 1999. The homeobox gene Phox2b is essential for the development of autonomic neural crest derivatives. Nature 399:366–370. [PubMed: 10360575]

Powley TL, Spaulding RA, Haglof SA. 2011. Vagal afferent innervation of the proximal gastrointestinal tract mucosa: chemoreceptor and mechanoreceptor architecture. J Comp Neurol 519:644–660. [PubMed: 21246548]

Ratcliffe EM. 2011. Molecular development of the extrinsic sensory innervation of the gastrointestinal tract. Auton Neurosci 161:1–5. [PubMed: 21147045]

Ratcliffe EM, Fan L, Mohammed TJ, Anderson M, Chalazonitis A, Gershon MD. 2011a. Enteric neurons synthesize netrins and are essential for the development of the vagal sensory innervation of the fetal gut. Dev Neurobiol 71:362–373. [PubMed: 21485011]

Ratcliffe EM, Farrar NR, Fox EA. 2011b. Development of the vagal innervation of the gut: steering the wandering nerve. Neurogastroenterol Motil 23:898–911. [PubMed: 21851506]

Ratcliffe EM, Setru SU, Chen JJ, Li ZS, D'Autreaux F, Gershon MD. 2006. Netrin/DCC-mediated attraction of vagal sensory axons to the fetal mouse gut. J Comp Neurol 498:567–580. [PubMed: 16917820]

Smith-Thomas LC, Fawcett JW. 1989. Expression of Schwann cell markers by mammalian neural crest cells in vitro. Development 105:251–262. [PubMed: 2806124]

Wang HU, Chen ZF, Anderson DJ. 1998. Molecular distinction and angiogenic interaction between embryonic arteries and veins revealed by ephrin-B2 and its receptor Eph-B4. Cell 93:741–753. [PubMed: 9630219]

Wang X, Chan AK, Sham MH, Burns AJ, Chan WY. 2011. Analysis of the sacral neural crest cell contribution to the hindgut enteric nervous system in the mouse embryo. Gastroenterology 141:992–1002 e1001–1006. [PubMed: 21699792]

Wilm B, Ipenberg A, Hastie ND, Burch JB, Bader DM. 2005. The serosal mesothelium is a major source of smooth muscle cells of the gut vasculature. Development 132:5317–5328. [PubMed: 16284122]

Yntema CL, Hammond WS. 1954. The origin of intrinsic ganglia of trunk viscera from vagal neural crest in the chick embryo. J Comp Neurol 101:515–541. [PubMed: 13221667]

Young HM, Newgreen D. 2001. Enteric neural crest-derived cells: origin, identification, migration, and differentiation. Anat Rec 262:1–15. [PubMed: 11146424]

Highlights:

- A novel whole-mount immunohistochemical protocol reveals the developmental patterning of the enteric nervous system and enteric vasculature in fetal mice.
- Enteric neural crest-derived cell migration correlates with the development of the primary enteric vascular plexus.
- Enteric sympathetic nerves follow intestinal arteries to reach the gut and subsequently integrate with enteric ganglia.

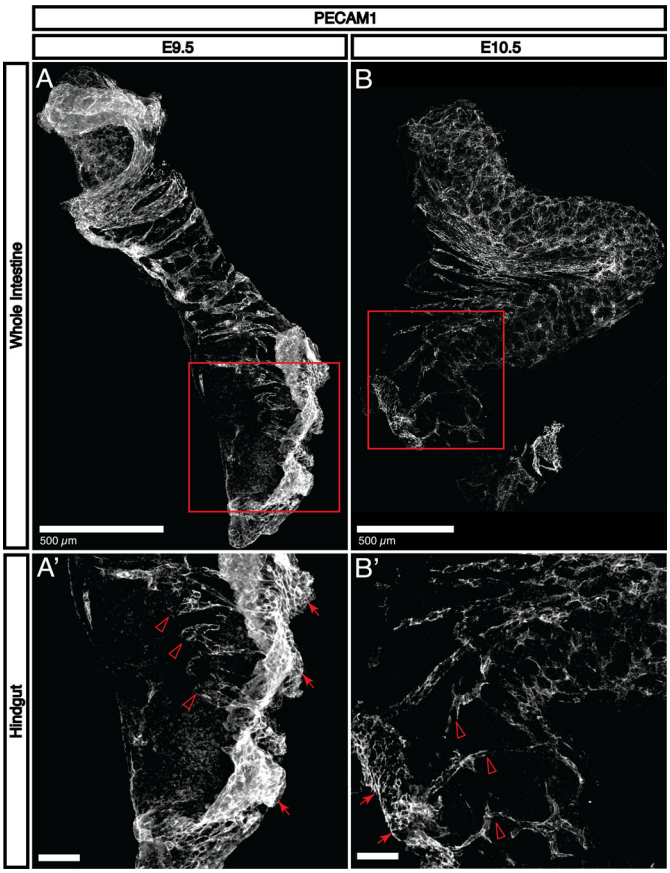

Fig. 1. Primary vascularization occurs immediately after tubulogenesis.

A-B: Immunohistochemical staining for PECAM1 shows that endothelial cells sprout into the intestine to form a primary capillary plexus between E9.5 and E10.5. At E9.5, only the proximal half of the intestinal tube has been significantly vascularized. By E10.5, the large intestine and small intestine begin to fold into apposition at the cecum, and the majority of both segments possess a recognizable capillary plexus. **A':** At E9.5, endothelial sprouts (open arrowheads) are clearly detectable adjacent to a large aggregation of PECAM1^{+} cells (arrows) that appears to be associated with the external mesoderm. **B':** By E10.5, only a few sprouts are visible in the most distal portions of the large intestine (open arrowheads). The PECAM1^{+} aggregation (arrows) is smaller and the signal intensity is reduced, suggesting that it may play a role only with primary vascularization.

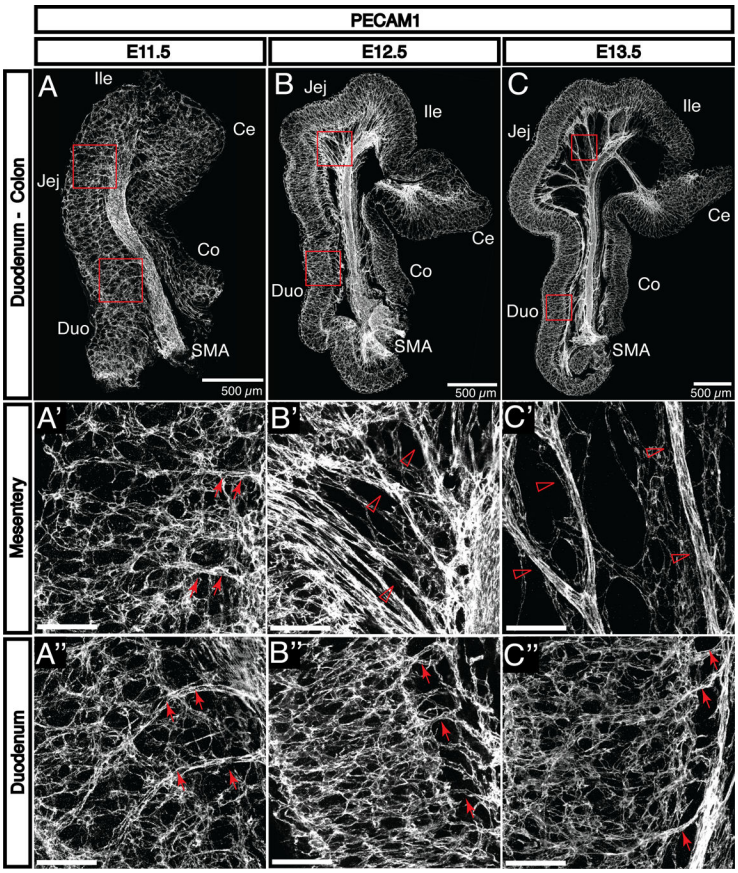

Fig. 2. The primary enteric capillary plexus is established at E11.5 and begins to remodel by E13.5.

A-C: PECAM1 staining reveals the development of embryonic vasculature in the small and large intestines from E11.5 to E13.5. **A'-A"**: The initial capillary plexus is uniform throughout the small intestine at E11.5. The mesentery is not yet detectable, and the superior mesenteric artery (SMA) is connected to the submucosal vascular plexus directly via capillaries (arrows). **B'**: As the gut tube lengthens at E12.5, it separates from the SMA to create the mesentery. The SMA is initially connected to the submucosal vasculature by smaller vessels (open arrowheads). **C'**: These vessels progressively remodel to form larger-diameter vessels which are observable by E13.5 (open arrowheads). **B"**: At E12.5 in the duodenum, the submucosal vasculature is connected to the mesenteric vasculature by small capillaries perpendicular to the length of the gut tube (arrows). **C"**: By E13.5, these vessels undergo a similar remodeling process to become recognizable as vasa recta (arrows). Notably, this process occurs first in the duodenum followed by the jejunum and the ileum. Duo, duodenum; Jej, jejunum; Ile, ileum; Ce, cecum; Co, colon. Scale bars = 100 μm except where indicated.

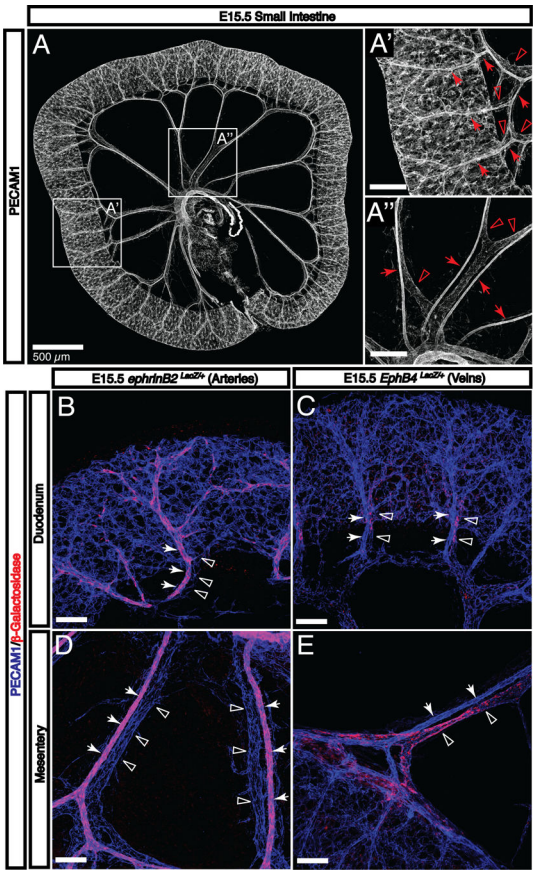

Fig. 3. Enteric arteries and veins adopt a stereotypical hierarchical pattern by E15.5.

A: By E15.5, the gut tube has completely separated from the SMA and the submucosal vasculature is connected to the SMA and SMV by both mesenteric vessels and vasa recta. **A'**: Vasa recta are readily apparent throughout the small intestine. These arteries (arrows) and veins (open arrowheads) are aligned and connect the submucosal vascular plexus with mesenteric vessels. **A"**: Mesenteric arteries (arrows) and veins (open arrowheads) are distinguishable by morphology. **B-E**: The expression of arterial (arrows) and venous (open arrowheads) molecular markers is visualized using *LacZ* reporter strains. Both types of vessels pattern adjacent to one another throughout intestinal development both in the mesentery and as they penetrate the gut wall. Scale bars = 100 μm except where indicated.

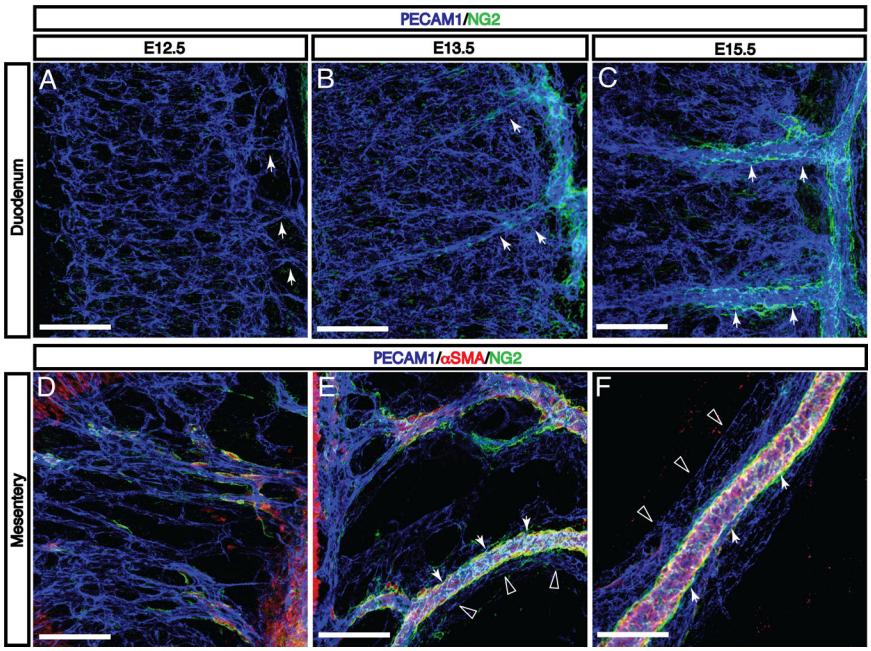

Fig. 4. Enteric vascular remodeling is correlated with recruitment of mural cells to intestinal arteries and vasa recta.

A: At E12.5, the onset of vascular remodeling, the submucosal vascular plexus is connected to the mesenteric vasculature by capillaries without detectable pericyte and vascular smooth muscle cell (VSMC) coverage. **B-C**: As these capillaries remodel to form vasa recta (arrows), $NG2^+$ mural cells are recruited to these large-diameter arteries. The submucosal vascular plexus remains largely free of coverage at E15.5. **D-F**: In the mesentery, αSMA^+ and/or $NG2^+$ mural cells first appear adjacent to the SMA at E12.5. As mesenteric capillaries remodel to form intestinal arteries and veins between E13.5 and E15.5, mural cells selectively surround arteries (arrows) but not veins (open arrowheads). Scale bars = 100 μm.

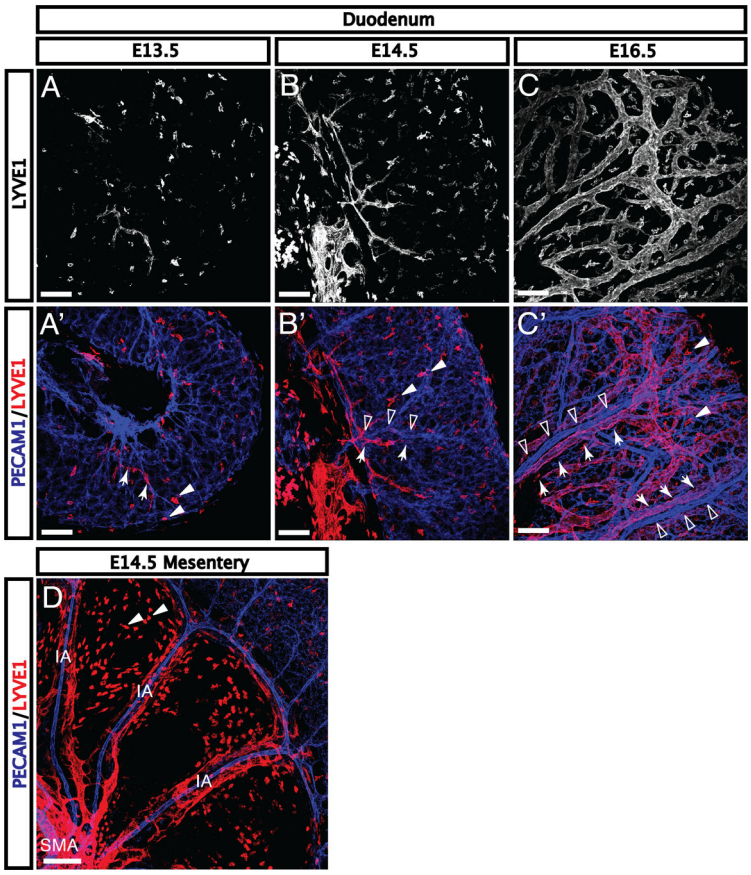

Fig. 5. Lymphatic vessels expand from the mesentery along veins beginning at E13.5.

A-A': LYVE1^{+} lymphatic vasculature is not detectable in the gut during the formation of the primary capillary plexus or at the onset of arterial and venous remodeling. The first LYVE1^{+} branches (red, arrows) appear in the duodenum at E13.5. **B-B'**: As more lymphatic vessels reach the submucosa around E14.5, sprouting lymphatic vessels (arrows) align with vasa recta (open arrowheads). **C-C'**: Upon reaching the gut wall, lymphatic proliferation quickly expands throughout the submucosal layer. Large lymphatic branches (arrows) can be found in close apposition with remodeled blood vessels (open arrowheads). (D) Lymphatic vasculature expands from the center of the mesentery outward along remodeled vessels to reach the gut, and aligns with vasa recta in the submucosa (IA, intestinal artery; SMA, superior mesenteric artery). Further, the appearance of lymphatics in the duodenum followed by the jejunum and ileum reflects the pattern of arterial and venous remodeling, suggesting that remodeled blood vessels may contribute to lymphatic patterning in the mesentery and submucosa. Note that LYVE1 expression is also detectable in tissue macrophages (arrowheads) from E13.5 onwards. Scale bars = 100 μm.

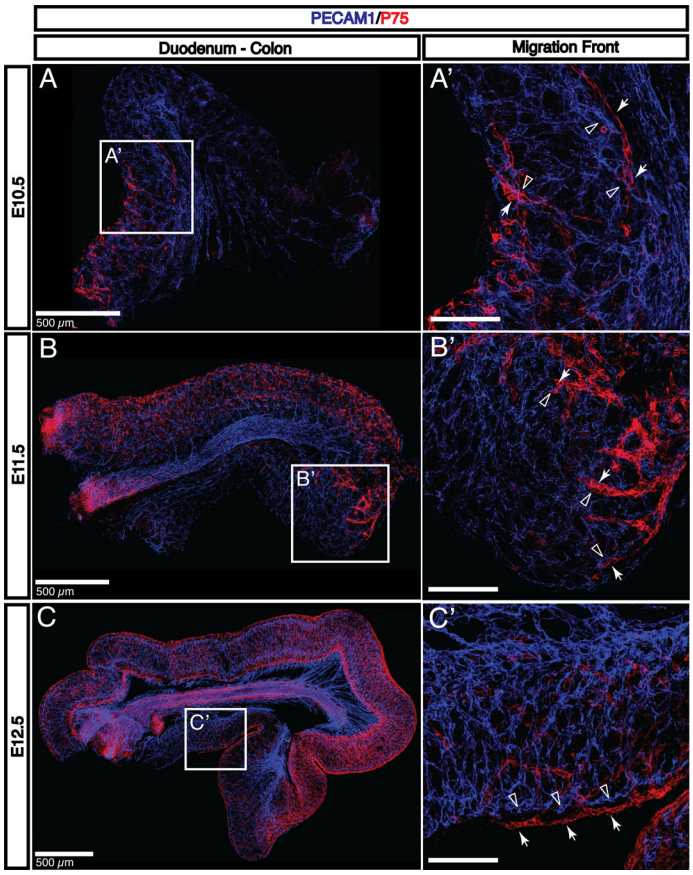

Fig. 6. Neural crest-derived cell migration is correlated with vasculogenesis, not angiogenesis.

A: P75^{+} neural crest-derived cells (NCDCs, red) arrive in the gut shortly following neovascularization to colonize the first half of the small intestine by E10.5. **B-C**: As the colonic capillary plexus is established at E11.5-E12.5, NCDCs continue their migration to reach the cecum by E11.5 and the distal portion of the colon at E12.5. A'-C': The migration front of NCDCs (red, arrows) never reaches a region without an established capillary plexus (blue, open arrowheads). Further, NCDCs are found closely adjacent to capillaries. However, despite the apparently close relationship between NCDCs and endothelial cells, higher magnification (C') reveals that NCDCs (arrows) migrate outside of the submucosal vascular layer and do not appear to directly contact endothelial cells (open arrowheads). Scale bars = 100 μm except where indicated.

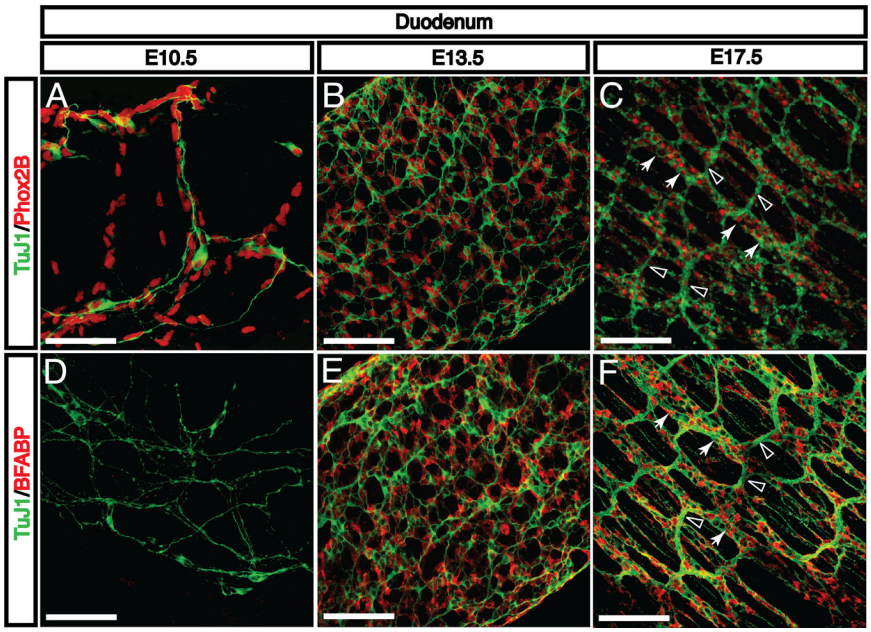

Fig. 7. Neural crest-derived cells differentiate into neurons and glia and organize into enteric ganglia.

A: During migration, some NCDCs express markers for neural progenitors such as Phox2b (red). At E10.5, only a small fraction of these progenitors express axonal markers characteristic of mature neurons, such as βIII tubulin (TuJ1, green). **B**: As NCDCs complete their migration by E13.5, all Phox2b^{+} neural cells are also TuJ1^{+}. At this stage, the ENS consists only of a uniform myenteric plexus without clear ganglia. **C**: By E17.5, neurons have reorganized into characteristic enteric ganglia (arrows) with interganglion axon bundles (open arrowheads). These ganglia are long and narrow, running perpendicular to the length of the gut tube. **D**: During early NCDC migration at E10.5, differentiated BFABP^{+} glial cells are not detectable (red). **E:** During the same E11.5-E13.5 period that neural progenitors begin to express axonal markers, glial cells become detectable and are evenly distributed throughout the E13.5 enteric nerve plexus. **F:** After reorganization of the enteric neural plexus to form ganglia, glial cells are found exclusively around enteric ganglia (arrows) and not axon bundles (open arrowheads) Scale bars = 100 μm.

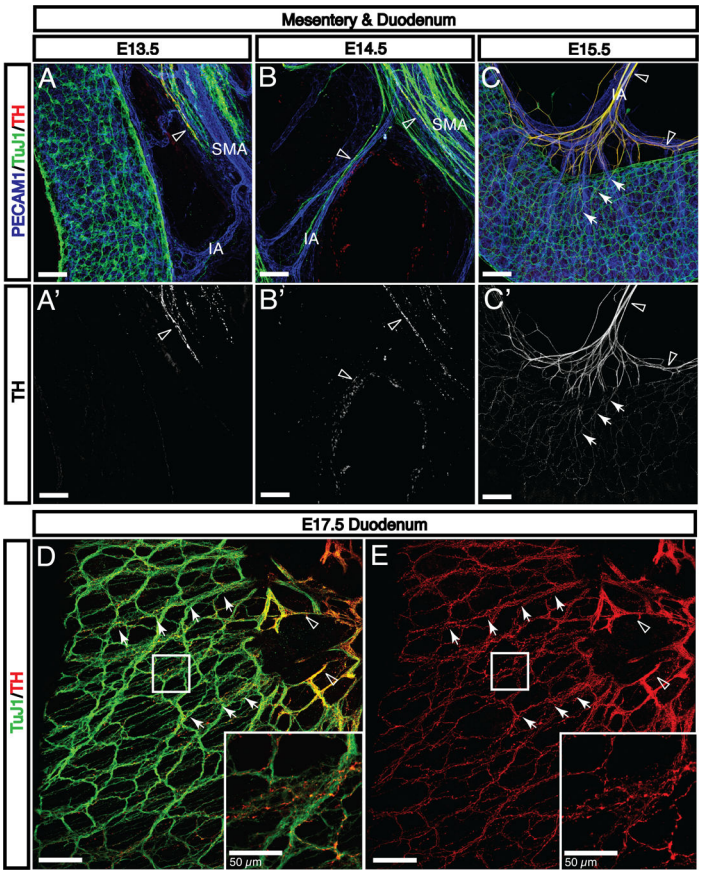

Fig. 8. Sympathetic axons follow intestinal arteries to reach the myenteric plexus prior to integrating with existing enteric nerves.

A-A': At E13.5, $TH^{+}/TuJ1^{+}$ sympathetic axons are found adjacent to the proximal region of the SMA (open arrowheads). **B-B'**: As angiogenic remodeling continues, these axons extend along intestinal arteries to reach the gut wall (open arrowheads). **C-C'**: Upon reaching the myenteric ENS plexus via the vasa recta, sympathetic axons rapidly defasciculate and follow existing enteric nerve bundles (arrows), suggesting that components of the ENS actively recruit sympathetic nerves (SMA, superior mesenteric artery; IA, intestinal artery). **D-E**: Sympathetic nerves rapidly extend throughout the ENS. Significant TH signals are found within every enteric ganglion (open arrowheads indicate sympathetic nerves aligned with arteries; arrows indicate sympathetic nerves aligned with enteric nerves). Sympathetic axon extension along unmyelinated axon bundles suggests that enteric neurons may be providing axon guidance cues. Scale bars = 100 μm except where indicated.

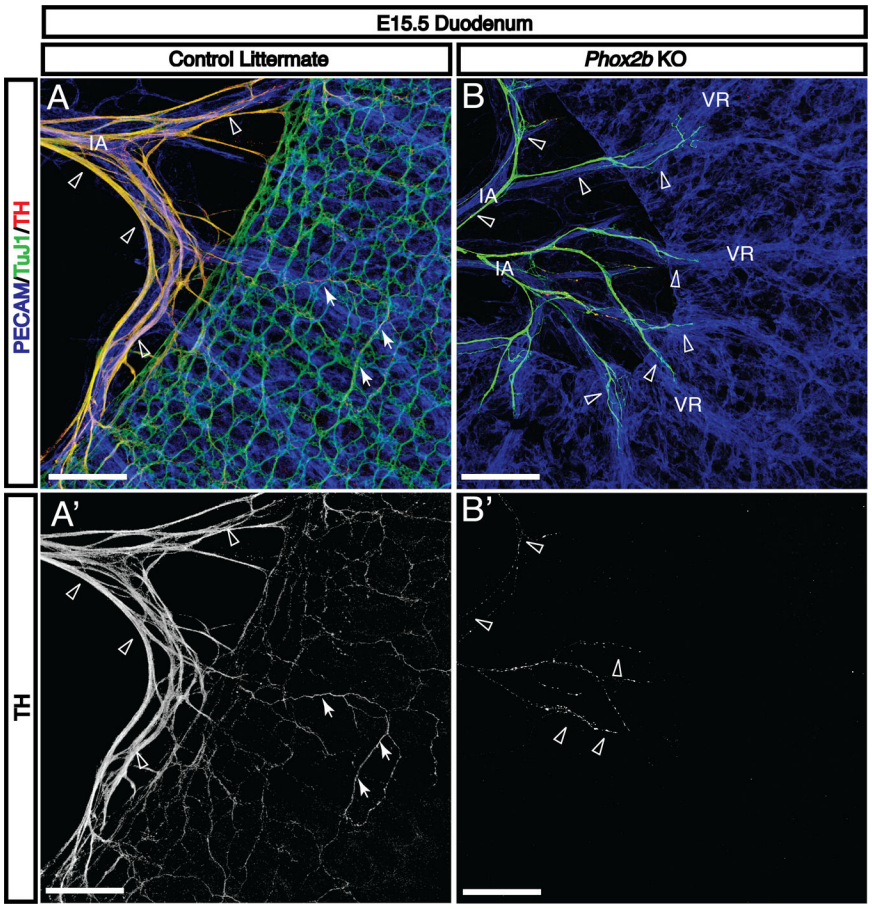

Fig. 9. In the absence of an ENS, sympathetic neurons continue to follow blood vasculature into the submucosa.

A-A': In wild-type littermates, TH^+ sympathetic axons follow intestinal arteries to reach the intestine (open arrowheads), and subsequently defasciculate to follow existing ENS nerve pathways in the subserosa (arrows). **B:** In *Phox2b*$^{-/-}$ mice, however, TH^+ sympathetic axons continue to follow arteries into the deeper submucosal plexus (open arrowheads). This observation suggests that vasa recta possess a capacity for axon guidance that is normally overridden by signals from the ENS. **B':** Reduced TH signal intensity in mutant embryos reflects the reduced number of sympathetic neurons in *Phox2b*$^{-/-}$ mice. IA, intestinal artery; VR, vasa recta. Scale bars = 100 μm.

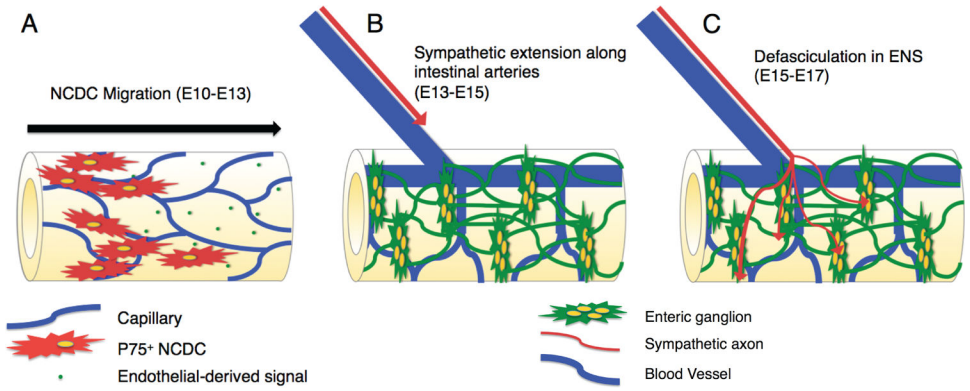

Fig 10. Proposed neurovascular interactions in NCDC migration and enteric sympathetic axon growth.

A: NCDCs migrate along the gut tube immediately following primary vascularization (E10-E13), and never enter a region of the gut prior to the development of a capillary plexus. As this migration occurs prior to angiogenic remodeling and NCDCs do not appear to directly contact capillary endothelial cells, we propose that these endothelial cells may secrete a soluble factor that promotes NCDC migration. **B:** Sympathetic innervation of the intestine requires two distinct axon guidance stages. From E13-E15, axons extend along intestinal arteries in the mesentery to reach the gut wall. VSMCs in arteries are likely to secrete guidance factors, as has been described in other tissues. **C:** Upon reaching the gut wall at E15, axons contact the ENS and rapidly spread throughout the enteric ganglia of the myenteric plexus by E17. Enteric neuron-derived netrins have been shown to guide vagal innervation, and a similar mechanism may influence sympathetic guidance within the ENS.

Table 1.

Primary antibodies used for whole-mount immunohistochemistry

Antigen	Host/Isotype	Manufacturer	Dilution
PECAM1	Hamster IgG	Chemicon	1:250
αSMA	Mouse IgG2a	Sigma	1:500
NG2	Rabbit Polyclonal	Dr. Bill Stallcup	1:200
ßIII-tubulin (TuJ1)	Mouse IgG2a	Covance	1:500
TH	Rabbit Polyclonal	Novus Biologicals	1:750
P75	Rabbit Polyclonal	Promega	1:500
Phox2b	Rabbit Polyclonal	Dr. Jean-Francois Brunet	1:500
BFABP	Rabbit Polyclonal	Dr. Thomas Muler	1:1000
LYVE1	Rabbit Polyclonal	Abcam	1:250
ß-galactosidase	Rabbit Polyclonal	MP Biomedicals	1:500